Received: 2 January 2021 | Revised: 24 March 2021 | Accepted: 28 March 2021

High Voltage

DOI: 10.1049/hve2.12105

ORIGINAL RESEARCH PAPER

# First-mode of negative streamers: Inception at liquid/solid interfaces

**David Ariza**[1] | **Abderrahmane Beroual**[2] | **Ralf Methling**[3] | **Sergey Gortschakow**[3] | **Harold R. Chamoro**[1]

[1]School of Electrical Engineering, KTH Royal Institute of Technology, Stockholm, Sweden

[2]Ecole Centrale de-Lyon, Ampère CNRS UMR 5005, Ecully, France

[3]Leibniz Institute for Plasma Science and Technology INP, Greifswald, Germany

**Correspondence**

David Ariza, School of Electrical Engineering, KTH Royal Institute of Technology, Stockholm, 10044, Sweden.
Email: dfag@kth.se

Associate Editor: Qing Yang

**Funding information**

SweGrids; InnoEnergy; German federal government (BMBF), Grant/Award Number: Research Programme 'Zukunftsfaehige Stromnetze', p; ABB Corporate Research

**Abstract**

An experimental study of the inception of the first-mode negative streamer at liquid/solid interfaces is presented in this article. The study is performed with a point-plane configuration under square high voltage pulses. The electrode configuration is immersed in mineral oil and the liquid/solid interface is assembled in contact with the point electrode or in its vicinity. Four polymers and two impregnated papers have been tested as solids of the liquid/solid interface. Thus, it is possible to compare the influence of different parameter of the solid and the interface on the streamer inception. For example: Permittivity, solid surface roughness, chemical composition, etc. It has been observed that streamer inception voltages at interfaces with solids of higher permittivity to that of the mineral oil are statistically similar. Additionally, streamer inception voltages of streamer initiated free in the oil (no liquid/solid interface) are similar to that of the inception voltage of cases with solids with high permittivity. In contrast, the inception voltage of streamers initiated at permittivity matched interfaces are shown to be highest of the cases. The streamer inception voltage is also studied for different distances between the liquid/solid interface and the point electrode with a permittivity matched interface. The results show a dependency of the inception voltage and the distance between the point electrode and the interface. Finally, an analysis of the observation is performed to show that the Townsend-Meek criterion cannot predict the obtained results.

## 1 | INTRODUCTION

Electrical pre-breakdown streamers phenomena in dielectric liquids is a complex process that involves different electronic, thermal and mechanical mechanisms [1]. The streamers phenomena in dielectric liquids are highly dependent on the experimental conditions [1, 2], such as the properties of the liquid, pressure, temperature, voltage, electrode configurations, etc. [1, 3]. One of the most common electrode arrangement to study the streamers is the point-plane electrode configuration [4]. It has been reported that streamers in a point-plane configuration with short electrode gaps (e.g. 5 mm) are also dependent on the curvature of the point electrode [5]. For instance, streamers initiated at point electrodes (positive and negative polarities) with radius of curvature between approximately 1 and 6 μm, are characterised by their slow velocity (~100 m/s) and irregular, but rounded, shape [5–8]. In negative polarity, this streamer type is usually referred to as first-mode negative streamer [2, 3, 6]. The inception of first-mode streamer has been usually observed at point electrodes with high electric fields (in the order of $10^7$ V/m). Usually, a current instability corresponding to an electron avalanche in the liquid phase initiated by free electrons at the tip is observed [1, 9, 10]. The rapid and localised injection of energy into the liquid produces a shock wave and the formation of a cavitation bubble [1, 10]. Under these conditions, the formed cavitation bubble is the precursor of the formation of first-mode negative streamers [1]. If series of successive discharges occur into the gaseous phase (with current pulses of ~100 μA peak and tens of nanoseconds duration), the cavitation bubble expands forming a streamer which expands until the last current pulse occurs. After the streamer propagation-expansion stops, it starts to implode and collapse [11]. The collapsing dynamics of the gaseous phase of the streamer has been also observed for other authors in [12, 13], describing the apparent collapse of the first mode negative streamer in long time periods.

Contrary to the described inception process in the liquid phase, the understanding of the inception process of the first-mode negative streamers at liquid/solid interfaces remains unclear. Note that dielectric solids are widely used in liquid-based insulation systems (e.g. power transformers, electrical bushings, power impregnated cables, capacitors etc). Therefore, there is a need to understand the physico-chemical processes involved in the streamer inception at these interfaces. Since, the inception mechanism of the first-mode of the negative streamer is better understood than for higher propagation modes (streamers with propagation velocity larger than 2 km/s) [2, 14–21], the experiments with first-mode negative streamers can provide valuable information of the influence of the interface in the streamer inception process and the formation of the cavity-bubble.

The inception of first-mode negative streamers at different liquid/solid interfaces (e.g. a point-plane electrode configuration with liquid/solid interface assembled in contact with the point electrode) can be affected by different parameters. For instance, the electric field at the point tip can be distorted and enhanced due to the permittivity mismatch of the liquid and the solid [22–25]. Furthermore, space charge accumulates on the solid surface, inducing electrostatic shielding of the field at the point electrode tip [22, 26]. Additionally, the interface restricts the volume where initiation of the streamers can take place [27]. Hence, further knowledge is required to clarify how the interface affects the streamer inception process and which properties of the solid can enhance or reduce the streamer inception probability.

This experimental study reports the streamer inception voltage probability of the first-mode negative streamers at mineral oil/solid interfaces. The solid samples investigated are one kraft paper, one paper made of micro and nano fibrils of cellulose and four polymer films which are polyethylene terephthalate (PET), low density polyethylene (LDPE), polyvinylidene fluoride (PVDF) and polytetrafluoroethylene (PTFE). In addition, a systematic study of the influence of the geometrical restriction enforced by the solid on the volume where the streamer can initiate is performed with a permittivity matched interface (mineral oil/PTFE). The obtained inception conditions for streamers creeping along permittivity matched and mismatched interfaces are also compared with existing theoretical criterion [28]. The results show that the existing streamer inception criterion is limited to predict the streamer inception conditions at mineral oil-solid interfaces.

## 2 | EXPERIMENTAL SETUP

A point-plane configuration is assembled inside of a test chamber. The radius of the point electrode $r_p$ is 2.9 μm. The plane electrode is made of a copper disk with 100 mm of diameter and covered with an impregnated paper (thickness of 100 μm) to prevent breakdown. The distance of the point-plane gap $d$ is fixed to 5 mm.

The investigated dielectric solid is placed inclined 60° to the plane electrode. The liquid/solid interface is assembled in contact with (or near) the point electrode tip, as shown in Figure 1. This configuration has been chosen such that the solid limits partially the high field volume in front of the tip where the initiation process of the streamer takes place.

A shadowgraphic system is used to acquire shadowgraphs of streamers initiated at the mineral oil/solid interface. The technique requires a light beam of a xenon lamp aligned with the point electrode tip, a far field microscope and a non-intensified high-speed camera. The detected image has a resolution of 1 μm per pixel. The shadowgraphic system is based on techniques reported in [2, 3, 11, 29–42]. A photon detection system based on an optical fibre and a photomultiplier is used to detect the light emission from the streamer.

A streamer charge measuring system based on a differential measurement technique using a third blunt electrode referred to as the probe electrode is used to detect the streamer charge. The probe electrode has similar construction as the point electrode. The probe electrode tip radius is 500 μm. The body of the probe and point electrodes are shield to inhibit stray capacitance. The bandwidth of the differential measurement system is 20 MHz with maximum sensitivity of 0.1 $pC$. The design of the streamer charge measurement system is based on [2, 35, 42–47]. A more detailed explanation of the experimental setup is already presented in [48, 49].

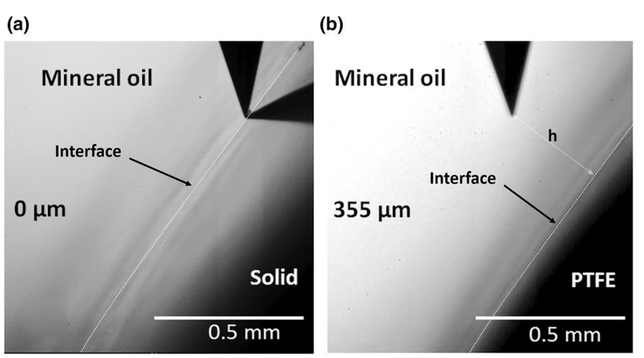


**FIGURE 1** Shadowgraph showing the assembled mineral oil/solid interface. (a) Solid surface assembled in contact with the point electrode tip and (b) Solid surface separated (355 μm) from the point electrode tip. PTFE, polytetrafluoroethylene

## 3 | SOLID SAMPLES

The sample of kraft paper is made of electrical grade unbleached kraft pulp (Munksjö AB, Aspa Bruk). The sample has been beaten for 4000 revolutions in a PFI-mill (mechanically treated). The second paper sample is the fibril paper. This sample is prepared from micro and nanofibrils of cellulose from kraft pulp. Note that the kraft fibrils preparations does not include chemical pre-treatment. The procedure consist in first beating the pulp 6000 revolutions in a PFI- mill and then homogenized it under a pressure of 1600 bar in a Microfluidiser M-110eh (Microfluidics Inc.). A Rapid Köthen sheet former (PTI) is used to prepare the kraft pulp fibres and the kraft fibrils according to procedures described in [50, 51].

A 3D optical profilometer (OptiTopo, RISE Bioeconomy, formerly Innventia AB) is used to measure the surface roughness of the kraft paper. The surface roughness of the other solid samples is measured with an atomic force microscope (AFM, Nanoscope IIIa AFM, Bruker AXS). Note that the definition of the average roughness of the AFM measurements is the root mean square of the values measured over three different areas (15 × 15 μm).

The polymer films used are polytetrafluoroethylene (PTFE FP301300), low density polyethylene (LDPE ET311201) polyvinylidene fluoride (PVDF FV301300) and polyethylene terephthalate (PET ES301400). Samples are supplied by Goodfellow Cambridge Ltd, Huntingdon, England. Parameters of the solids (relative permittivity and surface roughness) are summarised in Table 1. The thickness of the solid samples is 100 μm.

## 4 | PROCEDURE AND SOLIDS PREPARATIONS

### 4.1 | Oil and dielectric solid preparations

The preparation of the mineral oil previous to the electrical tests consists of the following procedure. The test chamber is filled with Nitro 10X (mineral oil). The oil level covers the point-plane electrodes. The filtering of the oil is done by pumping the oil in a closed loop composed by the test chamber, a hydraulic filter with pore size of 2 μm and the hydraulic pump. The degassing of the oil is done during the circulation in the closed loop. For this, the pressure of the test chamber is lowered to 5 mbar. When the oil returns to the test chamber it is poured on the surface of a heating rod which is at 60°C. This process aims to reduce possible air and moisture into the mineral oil. After 24 h of this process, dry air (80% nitrogen and 20% oxygen) is pumped into the test chamber. When the inner pressure of the test chamber reaches atmospheric pressure the mineral oil is cooled to room temperature.

**TABLE 1** Sample properties

| Material | Relative permittivity | Average surface roughness (nm) |
|---|---|---|
| LDPE | 2.2[a] | 30 |
| PET | 3.0[a] | 3 |
| PTFE | 2.0–2.1[a] | 130 |
| PVDF | 8.4 | 360 |
| Kraft fibril paper | 4.5[b] | 350 |
| Kraft paper | 3.2[b] | 2000 |
| Oil | 2.2[a] | - |

Abbreviations: LDPE, low density polyethylene; PET, polyethylene terephthalate; PTFE, polytetrafluoroethylene; PVDF, polyvinylidene fluoride.

[a]From supplier.

[b]Measured by dielectric spectroscopy [51].

The solid samples size is 8 × 100 mm. The samples preparations are done inside of a heated vacuum oven (5 mbar) at 105°C. These drying conditions remove moisture of the samples. The drying procedure for the LDPE is done at 70°C since it has low melting point. The drying process is done for 24 h. After it, the oven temperature is set to 60°C. Filtered mineral oil is pumped into the oven through a feed-through in a second glass container for degassing for 24 h. The degassed oil is poured on the solid sample for impregnation. Note that all process is done inside the closed oven.

### 4.2 | Testing procedure

The testing procedure is divided in two parts. In the first part, the solids are installed in contact with the point electrode as shown in Figure 1a. Thus, all solid samples produce the same spatial limitation of the volume where the streamer can initiate. After the sample is assembled, square high voltage pulses (rise time of 35 ns and duration of 40 μs) are applied to the electrode configuration. The range of the applied voltage is from 11.5 to 22 kV (steps voltage of approximately 0.6 kV). Four series of measurements were done. Each series has 10 measurements at the respective voltage level. There is 60 s of waiting between each voltage pulse. The selection of the peak voltage random to avoid memory effect in the experiment. In the second part, the streamer inception probability is studied for different distances between the point and the solid surface, ranging between 0 and 355 μm. This distance $h$ is set by moving the solid sideways, as it is shown in Figure 1. It is important to note that the point-plane gap distance $d$ has not been changed and remains 5 mm for all tests reported. This second part is only performed with the permittivity matched interface mineral-oil/PTFE. The measurements follow the procedure described above for the first part.

## 5 | EXPERIMENTAL RESULTS

### 5.1 | Streamer inception probability at mineral-oil/solid interfaces

The inception voltage probability is defined here by counting the streamers detected with the charge measuring system

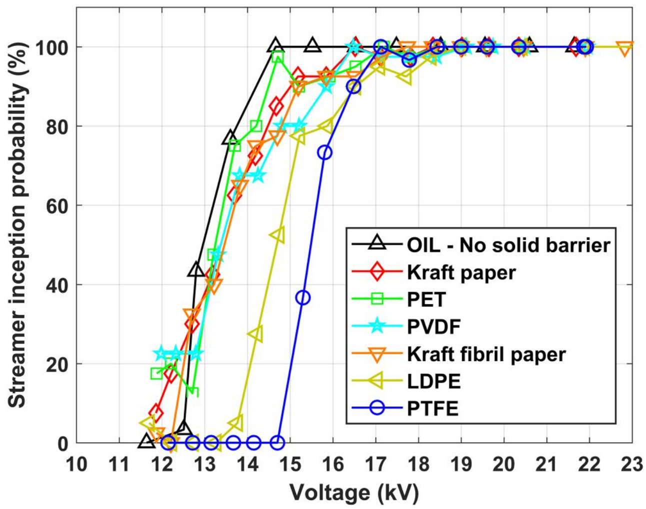


**FIGURE 2** Streamer inception probability for different mineral oil/solid interfaces tested. Point electrode tip in contact with the solid surface. LDPE, low density polyethylene; PET, polyethylene terephthalate; PTFE, polytetrafluoroethylene; PVDF, polyvinylidene fluoride

**TABLE 2** Inception voltage and its standard deviation for the streamers incepted at different interfaces in contact to the point electrode

| Material | Inception voltage $V_s$ (kV) | Standard deviation $\sigma$ (kV) |
|---|---|---|
| LDPE | 14.69 | 0.94 |
| PET | 13.23 | 0.59 |
| PTFE | 15.48 | 0.64 |
| PVDF | 13.48 | 1.45 |
| Kraft fibril paper | 13.31 | 1.30 |
| Kraft paper | 13.29 | 1.41 |
| Oil–without solid | 13.02 | 0.74 |

Abbreviations: LDPE, low density polyethylene; PET, polyethylene terephthalate; PTFE, polytetrafluoroethylene; PVDF, polyvinylidene fluoride.

(charge steps), photomultipliers (light pulses) and shadowgraphs for each voltage level. A streamer is assumed to be initiated if all three measuring systems detect the streamer. Figure 2 shows the probability distribution function of the inception voltage of streamers initiated with different mineral-oil/solid interfaces. The inception voltage probability is also reported for streamers without any solid barrier (reference case). Note that the obtained inception probability of the first mode negative streamers increases from 0% to 100% in a short interval of only 2 kV for all studied cases. This is typical observed in streamers initiated in negative polarity [42].

The 50% probability of streamer inception voltage in Figure 2 is hereinafter referred to as the inception voltage $V_s$ [38, 42]. The inception voltage and the standard deviation for each case are reported in Table 2. In order to determine whether the differences in $V_s$ are attributed to the stochastic nature of the streamer inception process, a statistical significance $t$-test is performed [52]. Considering a confidence level of 99.5%, it is found that the tests with PET, PVDF, kraft fibril paper, kraft paper and the reference case (no solid barrier) are statistically similar. Therefore, the small differences of their distribution functions can be attributed to the randomness of the phenomenon. In contrast, the inception voltages with LDPE and PTFE are statistically higher than in the cases without the solid barrier or with the cases with permittivity-mismatched interfaces. This shows that the LDPE and PTFE could have an impact on the streamer inception process. Since LDPE and PTFE match the permittivity of the mineral oil, no field intensification is expected to happen at the point tip due to the proximity of the interface. Thus, the low electric field intensification at the tip could be one of the reasons why the LDPE and PTFE have higher inception voltage than the other cases. However, the case with PVDF with very high permittivity do not show lower inception voltage than the other cases. This means, that not only field intensification can explain the obtained results. Probably, geometrical restrictions due to the presence of the solid can influence the streamer inception process. For instance, the position of the interface can obstruct the volume in front of the point electrode tip where the streamer can initiate. This volume obstruction can force the streamer initiation to have place on the side of the point electrode and not in front of the tip. In order to have a further understanding of the influence of the interface on the streamer inception process, an extended study of the mineral-oil/PTFE interface is presented in Section 5.2. Note that the study includes measurements for different distances between the point electrode and the interface. Thus, it is possible to detect if the volume obstruction influences the streamer inception process.

## 5.2 | Streamer inception probability at mineral-oil/PTFE interface

Figure 3 shows the streamer inception probability at the different distance h between the mineral-oil/PTFE interface and the point tip. The results without the solid barrier are also included in the figure and the streamer inception voltages are summarised in Table 3. Observe that the case without the solid barrier and with the PTFE surface in contact with the tip define the two extreme conditions of the test. As shown, the inception voltage of the mineral-oil/PTFE interface increases when the distance between the tip and the solid surface decreases. A Statistical $t$-tests (confidence level of 99.5%) shows that the inception voltage for the case with distance of 355 μm is similar to the test without the solid barrier. The cases reported with the solid in contact with the point electrode and the distances 5, 29 and 72 μm are found to be statistically different compared with the case without solid barrier. Therefore, the differences in the inception probability functions in Figure 3 can be attributed to the differences in the geometrical limitation of the streamer initiation by the presence of the PTFE interface.

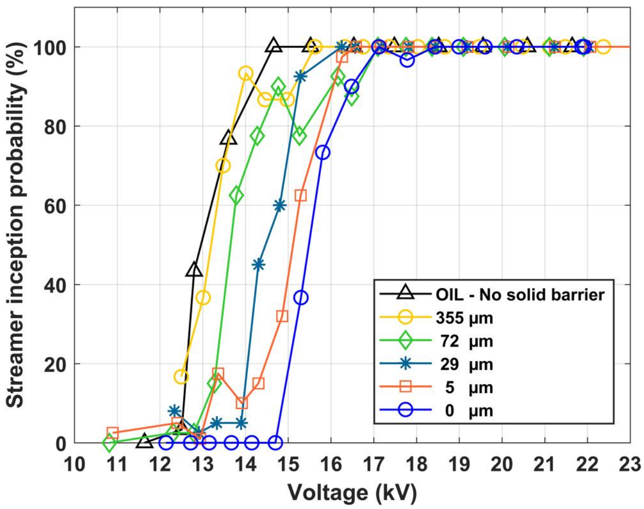


**FIGURE 3** Streamer inception probability at the mineral oil/PTFE interface at difference distances *h*. PTFE, polytetrafluoroethylene

**TABLE 3** Inception voltage and its standard deviation for the oil/PTFE interface for different distance *h*

| Distance *h* (μm) | Inception voltage $V_s$ (kV) | Standard deviation $\sigma$ (kV) |
|---|---|---|
| 0 | 15.48 | 0.64 |
| 5 | 15.16 | 0.78 |
| 29 | 14.44 | 0.82 |
| 72 | 13.73 | 0.51 |
| 355 | 13.27 | 0.70 |

Abbreviation: PTFE, polytetrafluoroethylene.

## 5.3 | Electron avalanche at the mineral-oil/PTFE interface

The electron avalanche in the liquid phase prior to the inception of a streamer is usually detected as a charge step of few pico coulombs in the charge recordings [42]. Figure 4 shows typical charge recordings for the mineral-oil/PTFE interface with distances between the point and the solid surface of 0, 4 and 8 μm when streamers are initiated at 15.5 kV. The measurements show an initial charge step, with not detectable light pulse correlated with it. This charge step is superimposed on a continuous component associated to conduction currents prior to the streamer initiation [38, 53]. The first charge step $q_f$ shown in Figure 4 corresponds to the integration of the detected current pulse produced by the electron avalanche in the liquid phase. A second charge step follows the initial charge step and a light pulse is correlated to it, which is generally attributed to a discharge inside the formed gaseous cavity. The average magnitude of $q_f$ for each distance case is reported in Table 4. It is not possible to distinguish between the first charge step $q_f$ and the second charge step correlated with a light pulse in all the measurements. Only about 40% of the measurements with detected streamers allowed a separation of both charge steps as shown in Figure 4. Since subsequent pulses of light correlated with the second charge step may appear soon after the development of the gaseous cavity [42], only events with a sufficient time $t_p$ between the charge steps can be detected.

The first charge step is delayed with time $t_q$ from the start of the voltage pulse. Similar features has been reported by other authors [42, 53]. This time delay usually is in the order of few hundred nanoseconds and decreases as the voltage is increased. The obtained time delay $t_q$ changes stochastically between a few hundreds of nanoseconds up to about three microseconds. This range is much larger than the time delay reported in [42]. This may be attributed to the presence of the solid.

The two charge steps cannot be distinguished anymore for distances between the point and the interface larger than 8 μm. Similar result is also observed for the solids of higher permittivity to that of the mineral oil, in contact with the point electrode. In this last case, the large number of subsequent pulses of light and steps of charge during the initiation of the streamer makes it impossible to distinguish $q_f$ in the charge recordings.

## 5.4 | Spatial limitation of the streamer with a solid of PTFE

Figure 5 shows the typical spatial limitation of streamers by the oil/PTFE permittivity matched interface for different distance *h* between the point electrode and the dielectric interface. Note that the corresponding streamer has a rounded irregular shape as in the case without barrier when the interface is located at a sufficiently long distance *h* (as far as 355 μm in Figure 5e). However, as *h* decreases, the solid limits the volume in front of the tip, forcing the growth of the streamer cavity along the interface. In that case, the shape of the gaseous cavity becomes elongated as the PTFE surface is brought closer to the tip. The gradual spatial limitation by the solid shown in Figure 5 clearly illustrates the geometrical difference of the zone where streamers can initiate as the distance *h* decreases.

# 6 | DISCUSSION

As mentioned before, the development of the first mode negative streamer relies in the generation of a gaseous cavity resulted from the energy dissipated of an electron avalanche (nanosecond duration) in the liquid [2, 11, 42]. In a point-plane configuration, the electron avalanche penetrates a distance *xi* from the point electrode (cathode) into the liquid. The penetration depth is estimated to be in the same order of magnitude as the tip radius $r_p$ [1, 9, 54]. The electron avalanche is expected to stop then at the distance where the electric field in front of the point reaches the minimum critical electric field $E_c$ required for electron multiplication.

The inception of streamers occur at a voltage $V_s$ when the electric field at the tip reaches the threshold initiation field $E_s$ [1]. However, $E_s$ is not a constant value characteristic only of

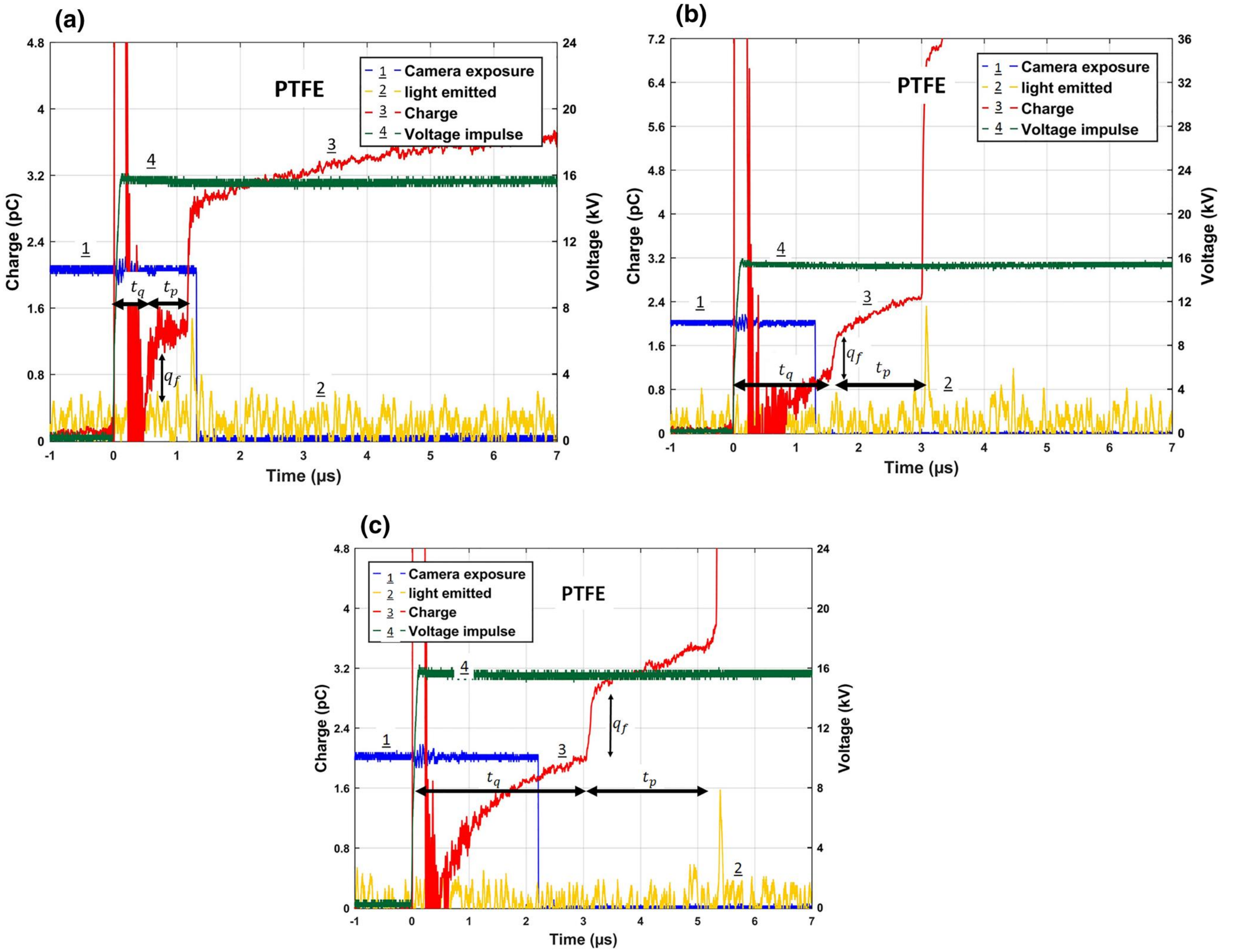


**FIGURE 4** Typical charge and light recordings of streamers initiating at the mineral oil-PTFE interface with three distances $h$. Note that the applied voltage corresponds to the inception voltage in each case. PTFE, polytetrafluoroethylene

**TABLE 4** Average charge of the electron avalanche $q_f$

| Distance ($\mu$m) | Charge ($pC$) |
|---|---|
| 0 | 0.5 |
| 4 | 0.7 |
| 8 | 0.9 |

the liquid since it also depends on electrode geometric parameters affecting the field distribution in front of the point [6]. Finite element calculations show that $E_s$ for the here-reported experiments in mineral oil without solid barrier is about 11 MV/cm. This field is similar to the values reported in [1, 6] for mineral oil. However, it is found experimentally that the initiation field $E_s$ increases with the permittivity of the solid barrier, as shown in Table 5. Moreover, $E_s$ also changes with the distance $h$ for the PTFE barrier (Table 6) even if there is no change in the field distribution in front of the point in these cases.

Since the initiation tip field $E_s$ in this experiment is not constant for the different studied solid barriers, a more elaborated analysis of the streamer inception is required. Based on the demonstrated existence of an electronic avalanche occurring in the liquid phase for negative streamer initiation [6, 11, 42, 55], theoretical efforts to estimate the inception voltage $V_s$, assume a similar physical process as that causing the initiation of streamer discharges in hydrocarbon gases (e.g. [28]). Thus, the streamer is incepted in the liquid when a single electron avalanche reaches a critical size $N_{cr}$. According to [1, 7], the growth of a single electron avalanche can be described as:

$$n_e = n_0 \exp\left(\int_0^{xi} \alpha(E(x), \rho_l)dx\right) \quad (1)$$

where $n_e$ is the number of electrons generated during the development of an avalanche, $n_0$ is the number of electron initiating the electron avalanche and $xi$ is the penetration

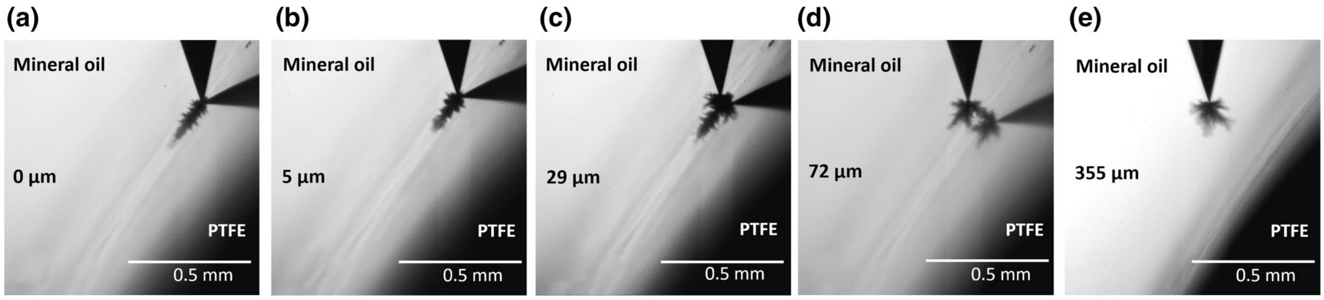


**FIGURE 5** Shadowgraph of the first-mode negative streamer at the mineral oil/PTFE interface. The shadowgraphs show experiments at five gap distances from the point electrode tip to the PTFE solid surface. The solid surface is inclined 60° to the plane electrode. The applied voltage is 22 kV in each shadowgraph. $r_p$ = 2.9 µm, $d$ = 5 mm. PTFE, polytetrafluoroethylene

**TABLE 5** Comparison of the experimental tip field and estimation of the streamer inception criterion (3) for the tested mineral-oil/solid interfaces in contact with the point tip

| Distance ($\mu$m) | Theoretical estimations for $K_{cr}$ = 15.7 | | Experimental value $E_s$ (MV/cm) |
|---|---|---|---|
| | $V_s$ (kV) | $E_s$ (MV/cm) | |
| -(Without solid) | 13 | 11.1 | 11.1 |
| PTFE | 13.1 | 11.1 | 13.0 |
| LDPE | 13.2 | 11.2 | 12.5 |
| PET | 12.7 | 12.5 | 13.0 |
| Kraft paper | 12.6 | 13.1 | 13.8 |
| Kraft fibril paper | 11.6 | 16.3 | 18.6 |
| PVDF | 7.95 | 19.7 | 33.4 |

Abbreviations: LDPE, low density polyethylene; PET, polyethylene terephthalate; PTFE, polytetrafluoroethylene; PVDF, polyvinylidene fluoride.

**TABLE 6** :Comparison of the experimental tip field and estimatation of the streamer inception criterion (3) for a permittivity matched interface for different distances $h$

| Distance ($\mu$m) | Theoretical estimations for $K_{cr}$ = 15.7 | | Experimental value $E_s$ (MV/cm) |
|---|---|---|---|
| | $V_s$ (kV) | $E_s$ (MV/cm) | |
| -(Without solid) | 13.0 | 11.1 | 11.1 |
| 355 | 13 | 11.1 | 11.3 |
| 72 | 13 | 11.1 | 11.6 |
| 29 | 13 | 11.1 | 12.2 |
| 5 | 13.1 | 11.1 | 12.8 |
| 0 | 13.1 | 11.1 | 13.0 |

depth. $\alpha$ is the electron collision ionization coefficient of the liquid which depends on the fluid density $\rho_l$ and the field distribution near to the point electrode $E(x)$, where $E_c < E(x) < E_s$. This ionization coefficient can be expressed as [28]:

$$\alpha = A_l\rho_l \exp(B_l\rho_l/E(x)) \tag{2}$$

where, the coefficients $A_l\rho_l$ (in $10^6$ cm$^{-1}$) and $B_l\rho_l$ (in MV cm$^{-1}$) are characteristic values of the liquid respectively. Typical values of these coefficients for hydrocarbon liquids are 1.1 and 18 for hexane, 1.3 and 19 for cyclohexane, and 1.2 and 18 for pentane as reported in [28].

Rewriting Equation (1), the criterion for the inception of streamers can be obtained as [28]:

$$\int_0^{xi} \alpha(E(x),\rho_l)dx = \ln\left(\frac{n_e}{n_o}\right) = K_{cr} \tag{3}$$

where the integral of the ionization coefficient is a dimensionless parameter $K$ that typically ranges between 5 and 20 [28].

In order to compare the results presented in Section 5 with the streamer inception criterion condition (3), the coefficients $A_l\rho_l$ and $B_l\rho_l$ of mineral oil are required. Unfortunately, these coefficients are not known for mineral oil. Thus, the coefficients $A_l\rho_l$ and $B_l\rho_l$ of cyclohexane are here used as a rough model of Nitro 10X since alkanes are the major component of mineral oil [56].

Note that Equation (3) can be also expressed in terms of the charge of the electron avalanche $q_f = n_e q$, the initialising electrons $q_0 = n_0 q$ and the fundamental charge of an electron $q$, as shown in Equation (4):

$$\ln\left(\frac{q_f}{q_o}\right) = K_{cr} \tag{4}$$

Assuming that the electron avalanche is initiated by only one electron $q_0$ = -1.602 × $10^{-19}$ C and the charge of the electron avalanche $q_f$ = 0.7 pC as the average of the measured values reported in Table 4, a rough estimation of $K_{cr} \approx 15.7$ can be obtained. Thus, a streamer is initiated in the liquid phase when the ionization integral of the electron avalanche exceeds the critical number $K_{cr}$ [28]. Therefore, the obtained $K_{cr}$ is used for the evaluation of the streamer inception in all the cases reported in the previous section.

A 2D model has been developed in COMSOL to make the calculation of the streamer criteria (3) for the studied cases in this article. The 2D model represents the point-plane arrangement and the solid with the geometry conditions described in the Sections 2 and 3 to create the liquid/solid interface. Figure 6 shows a close detail of the obtained simulations near to the point electrode for some of the cases. The 2D calculations follows the calculation method proposed in [57].

A summary of the calculated inception voltages and electric fields that satisfy the streamer inception criteria $K_{cr}$ for each solid case are presented in Table 5. The streamer inception criterion (3) predicts a decreasing $V_s$ as the permittivity of the solid increases. Nevertheless, the experimental results presented in Table 2, show that the streamer inception voltage remains rather constant in the case of the permittivity-mismatched interfaces. Additionally, the predicted $E_s$ from streamer inception criterion is lower than the obtained initiation electric field at the respective inception voltage $V_s$ from the experiments as shown in Tables 2 and 5. This is especially evident in the case with PVDF which has the highest permittivity of all the tested solids.

For the permittivity-matched interface of mineral oil/PTFE studied in Section 5.2, the experimental results show that the streamer inception voltage increases from 13.3 to 15.5 kV by reducing the distance $h$. However, the streamer inception criteria (3) does not predict such an increment in $V_s$ as shown in Table 6. Additionally, the electric field at the point electrode calculated with the streamer inception criterion remains constant by decreasing $h$. Nevertheless, the $E_s$ obtained from measurements tend to increase by decreasing $h$.

Thus, Tables 5 and 6 show that the criterion proposed in [28] may have some limitations to estimate the streamer inception conditions for the here-reported experiments with mineral oil/solid interfaces. However, the lack of parameters $A_l\rho_l$ and $B_l\rho_l$ of mineral oil does not allow to conclude if the criteria (3) is suitable or not. In order to illustrate the electrostatic conditions at the inception voltage $V_s$ for some of the tests performed, the electric field distributions for the tests without solid and with the PTFE and PVDF films are shown in Figure 6. The red-brown line is the equipotential line at which the electric field intensity is equal to 6 MV/cm. This point is defined few micrometers far from the tip and defines the assumed critical electric field $E_c$ where the ionization coefficient (4) becomes significant. As it can be seen, the size of the volume where avalanches can be generated in the oil at the measured $V_s$ is different in each case. Moreover, observe that the path (shown in dashed lines) followed by the strongest avalanche in the presence of an interface is also strongly dependent on the permittivity of the solid used. Thus, Figure 6 shows that the maximum size of the avalanches that can be generated in the liquid phase is not constant at $V_s$ and therefore it cannot be uniquely used to define the streamer inception.

On the other hand, the estimated maximum penetration depth in the cases shown in Figure 6 does not exceed more than few micrometres. This depth is in the same order of magnitude as the tip radius $r_p$, in agreement with [1, 2, 9, 54]. For this reason, it is expected that the avalanche zone is geometrically limited when an interface is located at a shorter distance $h$ than the penetration depth. This effect would result in a reduction of the avalanche charge when reducing $h$, which is in qualitative agreement with the values reported in Table 4 for the PTFE interface. Furthermore, it could be possible to assume that the reduction of the charge of the electron avalanche due to spatial limitation leads to an immediate compensation in energy requiring a higher inception field $E_s$ as it is reported in Table 6. Nevertheless, the tests with the PTFE film also show that the inception voltage can be affected by the interface located at a distance $h$ larger than the avalanche penetration depth. Thus, this effect cannot be predicted by evaluating the size of avalanches in front of the point tip as assumed in [28].

Since the formation of an avalanche is a necessary, but not the only condition for streamer initiation, later processes (such as the formation and expansion of the cavity or the discharges in the gas phase) may actually define the threshold for

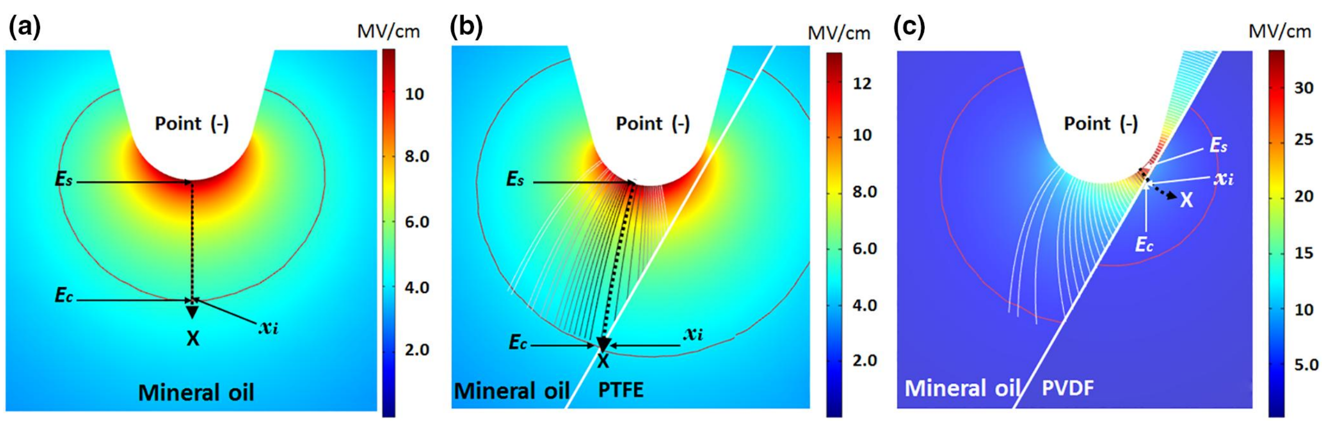


**FIGURE 6** Electric field distribution and evaluation of the electron concentration at the inception voltage for: (a) no solid barrier case at $V_s$ = 13.02 kV, (b) mineral oil/PTFE barrier at $V_s$ = 15.48 kV and (c) Mineral oil/PVDF interface at $V_s$ = 13.48 kV. $r_p$ = 2.9 µm, $d$ = 5 mm. PTFE, polytetrafluoroethylene; PVDF, polyvinylidene fluoride

inception in the presence of a solid material. Interestingly, Table 3 shows that the interface can increase $V_s$ even under distances $h$ larger than several tens of micrometres. Unfortunately, this result is difficult to explain based on the current understanding of streamers in dielectric liquids.

## 7 | CONCLUSION

The experimental study shows two remarkable features of the streamer inception at mineral oil/solid interfaces: First, the inception voltages are found to be statistically similar for the cases without the solid barrier and the cases of interfaces with solids of permittivity higher than that of the liquid. Additionally, the electric field intensification at the point electrode because of permittivity mismatch of the interface, does not result in significant changes of the streamer inception voltage. Second, the cases with solids made of PTFE and LDPE (no permittivity mismatch of the interface) have higher inception voltage than the case without a solid barrier. The systematic study of the streamer inception at the mineral oil/PTFE interface indicates that the inception voltage increases by decreasing the gap between the solid surface and the point electrode. The maximum streamer inception voltage is obtained when the PTFE surface is in contact with the point electrode. In addition, the detected charge step $q_f$ (electron avalanche) increases slightly if the interface is separated from the point electrode. The systematic evaluation of the streamer inception criteria with permittivity matched and mismatched interfaces shows that the streamer inception criteria based only in a critical charge multiplication number seems to be limited to predict correctly the inception voltage and electric field in mineral oil/solid interfaces. Additionally, the observation suggests that not only high field conditions at the point electrode tip are needed to initiate a streamer, but also enough space between the solid surface and the point electrode. Since the inception process in negative polarity is related to the formation of a gaseous cavity, it is important to understand if differences in the wettability of the solids can enhance the gaseous cavity formation at the interface. Therefore, it is suggested to study this condition in the future work. It is also proposed to study in the future work the influences of the inclination of the solid. It is important to understand if geometrical restrictions influences the space charge accumulation at the interface even under very short rise times.

## ACKNOWLEDGMENTS

The authors acknowledge the financial support of ABB AB Corporate Research, the Swedish Centre for Smart Grids and Energy Storage SweGRIDS, the EIT Innoenergy Materials platform, the Swedish Energy Agency through the Elforsk program and the Walleenberg Wood Science Center. The research presented in this paper was also supported by German Federal Government (BMBF) in the frames of the 6. Federal Research Programme 'Zukunftsfaehige Stromnetze', project 03SF0476.

## ORCID

*David Ariza* https://orcid.org/0000-0002-4800-9990

## REFERENCES


1. Denat, A.: High field conduction and prebreakdown phenomena in dielectric liquids. IEEE Trans. Dielectr. Electr. Insul. 13(3), 518–525 (2006)
2. Lesaint, O.: Prebreakdown phenomena in liquids: propagation modes and basic physical properties. J. Phys. Appl. Phys. 49(14) (2016). 144001
3. Beroual, A., et al.: Propagation and structure of streamers in liquid dielectrics. IEEE Electr. Insul. Mag. 14(2), 6–17 (1998)
4. Coelho, R., Debeau, J.: Properties of the tip-plane configuration. J. Phys. Appl. Phys. 4(9), 305 (1971)
5. Yamashita, H., Yamazawa, K., Wang, Y.S.: The effect of tip curvature on the prebreakdown streamer structure in cyclohexane. IEEE Trans. Dielectr. Electr. Insul. 5(3), 396–401 (1998)
6. Lesaint, O., Top, T.V.: Streamer initiation in mineral oil. Part I: electrode surface effect under impulse voltage. IEEE Trans. Dielectr. Electr. Insul. 9(1), 84–91 (2002)
7. Yasui, Y., Yamazawa, K., Yamashita, H.: The local field distribution in the vicinity of needle tip under the existence of streamer. In: Proceedings of 1999 IEEE 13th International Conference on Dielectric Liquids (ICDL'99) (Cat. No.99CH36213), pp. 118–121. Nara (1999)
8. Lesaint, O., Jung, M.: On the relationship between streamer branching and propagation in liquids: influence of pyrene in cyclohexane. J. Phys. D Appl. Phys. 33(11), 1360–1368 (2000)
9. Haidara, M., Denat, a.: Electron multiplication in liquid cyclohexane and propane. IEEE Trans. Electr. Insul. 26(4), 592–597 (1991)
10. Kattan, R., Denat, A., Bonifaci, N.: Formation of vapor bubbles in nonpolar liquids initiated by current pulses. IEEE Trans. Electr. Insul. 26(4), 656–662 (1991)
11. Kattan, R., Denat, A., Lesaint, O.: Generation, growth, and collapse of vapor bubbles in hydrocarbon liquids under a high divergent electric field. J. Appl. Phys. 66(9), 4062–4066 (1989)
12. Lundgaard, L., et al.: Pre-breakdown phenomena in hydrocarbon liquids in a point-plane gap under step voltage. Part 2: Behaviour under negative polarity and comparison with positive polarity. J. Phys. Commun. 4(4), 045011
13. Sékongo B., et al.: Temperature dependence of the pre-breakdown and breakdown phenomena in natural esters under AC stress. IET Science, Measurement & Technology. 14(9), 762–769 (2020)
14. Sitorus, H.B., et al.: Creeping discharges over pressboard immersed in jatropha curcas methyl ester and mineral oils. In: 2015 IEEE 11th International Conference on the Properties and Applications of Dielectric Materials (ICPADM), pp. 152–155. IEEE, Sydney (2015)
15. Kebbabi, L., Beroual, A.: Fractal analysis of creeping discharge patterns propagating at solid/liquid interfaces - influence of the nature and geometry of solid insulators. In: CEIDP '05. 2005 Annual Report Conference on Electrical Insulation and Dielectric Phenomena, vol. 2005, pp. 132–135. Nashville. IEEE (2005)
16. Beroual, A., et al.: Analysis of creeping discharges activity at solid/liquid interfaces subjected to ac voltage. IET Gener., Transm. Distrib. 5(9), 973 (2011)
17. Beroual, A., Kebbabi, L.: Influence of the voltage waveform and hydrostatic pressure on morphology and final length of discharges propagating over solid-liquid interfaces. IEEE Trans. Dielectr. Electr. Insul. 16(6), 1574–1581 (2009)
18. Beroual, A., Kebbabi, L.: Influence of hydrostatic pressure on morphology and final length of creeping discharges over solid/liquid interfaces under impulse voltages. In: 2008 IEEE International Conference on Dielectric Liquids, Chasseneuil, pp. 1–4. IEEE (2008)
19. Beroual, A., Kebbabi, L.: Influence of capacitive effects on the characteristics of creeping discharges propagating over solid/liquid interfaces under impulse voltages. In: 2008 Annual Report Conference on Electrical Insulation and Dielectric Phenomena, pp. 357–360. IEEE, Quebec (2008)
20. Beroual, A., et al.: Investigation on creeping discharges propagating over pressboard immersed in mineral and vegetable oils under AC, DC and

lightning impulse voltages. IEEE Trans. Dielectr. Electr. Insul. 20(5), 1635–1640 (2013)
21. Lundgaard, L., et al.: Propagation of positive and negative streamers in oil with and without pressboard interfaces. IEEE Trans. Dielectr. Electr. Insul. 5(3), 388–395 (1998)
22. Yi, X.: Characteristics of creepage discharges along ester-pressboard interfaces under ac stress. Ph.D. dissertation, University of Manchester, Manchester (2012)
23. Yi, X., Wang, Z.: Surface tracking on pressboard in natural and synthetic transformer liquids under AC stress. IEEE Trans. Dielectr. Electr. Insul. 20(5), 1625–1634 (2013)
24. Yi, X., et al.: Surface treeing on pressboard barriers in synthetic and natural ester liquids under AC stress. In: Proceedings of the IEEE International Conference on Dielectric Liquids, pp. 48–51. Trondheim (2011)
25. Taylor, R.J.: Effect of permittivity matching on the flashover of solid/liquid interfaces. Proc. Inst. Electr. Eng. UK. 124(10), 899 (1977)
26. Liu, Q., et al.: Accumulative effect on streamer propagation of lightning impulses on oil/pressboard interface. In: Proceedings of the IEEE International Conference on Dielectric Liquids, pp. 1–4. Trondheim (2011)
27. Liu, Q., Wang, Z.: Streamer characteristic and breakdown in synthetic and natural ester transformer liquids with pressboard interface under lightning impulse voltage. IEEE Trans. Dielectr. Electr. Insul. 18(6), 1908–1917 (2011)
28. Naidis, G.V.: On streamer inception in hydrocarbon liquids in point-plane gaps. IEEE Trans. Dielectr. Electr. Insul. 22(5), 2428–2432 (2015)
29. Nieto-Salazar, J., Lesaint, O., Denat, A.: Transient current and light emission associated to the propagation of pre-breakdown phenomena in water. In: 2003 Annual Report Conference on Electrical Insulation and Dielectric Phenomena, pp. 542–545. IEEE, Albuquerque (2003)
30. Costeanu, L., Lesaint, O.: On mechanisms involved in the propagation of subsonic positive streamers in cyclohexane. In: Proceedings of the 2002 IEEE 14th International Conference on Dielectric Liquids (ICDL), pp. 143–146. IEEE, Graz (2002)
31. Yamashita, H., et al.: The effect of high pressure on prebreakdown phenomena in n-hexane. In: Proceedings of the 10th International Conference on Conduction and Breakdown in Dielectric Liquids, pp. 404–409. IEEE, Grenoble (1990)
32. Unge, M., et al.: Enhancements in the lightning impulse breakdown characteristics of natural ester dielectric liquids. Appl. Phys. Lett. 102(17), 172905 (2013)
33. Nakao, Y., et al.: Propagation characteristics of impulse creepage discharge in a parallel-plane gap with a protruding point in transformer oil. Electr. Eng. Jpn. 124(2), 1–7 (1998)
34. Lesaint, O., Massala, G.: Positive streamer propagation in large oil gaps: experimental characterisation of propagation modes. IEEE Trans. Dielectr. Electr. Insul. 5(3), 360–370 (1998)
35. Sitorus, H.B., et al.: Comparison of streamers characteristics in jatropha curcas methyl ester oil and mineral oil under lightning impulse voltage. In: Proceedings of the 2014 IEEE 18th International Conference on Dielectric Liquids (ICDL), Bled, 1–4 (2014)
36. Duy, C., et al.: Streamer propagation and breakdown in natural ester at high voltage. IEEE Trans. Dielectr. Electr. Insul. 16(6), 1582–1594 (2009)
37. Ingebrigtsen, S., Lundgaard, L.E., Åstrand, P.-O.: Effects of additives on prebreakdown phenomena in liquid cyclohexane: II. Streamer propagation. J. Phys. D Appl. Phys. 40(18), 5624–5634 (2007)
38. Ingebrigtsen, S., Lundgaard, L.E., Åstrand, P.-O.: Effects of additives on prebreakdown phenomena in liquid cyclohexane: I. Streamer initiation. J. Phys. D Appl. Phys. 40(17), 5161–5169 (2007)
39. Gournay, P., Lesaint, O.: On the gaseous nature of positive filamentary streamers in hydrocarbon liquids. II: propagation, growth and collapse of gaseous filaments in pentane. J. Phys. D Appl. Phys. 27(10), 2117–2127 (1999)
40. Ohgaki, S., Tsunoda, Y.: A study of the positive streamer growth under surface discharge configuration in liquid paraffin. IEEE Trans. Electr. Insul. EI-19(6), 594–601 (1984)
41. Dumitrescu, L., et al.: Study of streamer inception under impulse voltage in liquid cyclohexane. In: Proceedings of the 2000 Annual Report Conference on Electrical Insulation and Dielectric Phenomena (Cat. No.00CH37132), Victoria, vol. 1, pp. 300–303. IEEE, Victoria (2000)
42. Dumitrescu, L., et al.: Study of streamer inception in cyclohexane with a sensitive charge measurement technique under impulse voltage. J. Electrost. 53(2), 135–146 (2001)
43. Beroual, A., Marteau, C., Tobazeon, R.: Measurement of the charge of a single or of a series of streamers in liquids subjected to a voltage step. IEEE Trans. Electr. Insul. 23(3), 427–431 (1988)
44. Sitorus, H.B.H., et al.: Pre-breakdown phenomena in new vegetable oil - based jatropha curcas seeds as substitute of mineral oil in high voltage equipment. IEEE Trans. Dielectr. Electr. Insul. 22(5), 2442–2448 (2015)
45. Dang, V.H., et al.: Streamer propagation in seed based insulating oils under lightning impulse voltages. In: Proceedings of the 2012 International Conference on High Voltage Engineering and Application (ICHVE 2012), pp. 659–662. Shanghai (2012)
46. Dang, V.H., Beroual, A., Perrier, C.: Comparative study of streamer phenomena in mineral, synthetic and natural ester oils under lightning impulse voltage. In: Proceedings of the 2010 International Conference on High Voltage Engineering and Application (ICHVE), pp. 560–563. New Orleans (2010)
47. Hestad, O., Lundgaard, L., Linhjell, D.: New experimental system for the study of the effect of temperature and liquid to solid transition on streamers in dielectric liquids: application to cyclohexane. IEEE Trans. Dielectr. Electr. Insul. 17(3), 764–774 (2010)
48. Ariza, D., et al.: First mode negative streamers along mineral oil-solid interfaces. IEEE Trans. Dielectr. Electr. Insul. 24(4), 2371–2382 (2017)
49. Ariza, D., et al.: Positive streamers: inception and propagation along mineral-oil/solid interfaces. J. Phys. Commun. 4(2), 025008 (2020)
50. Sehaqui, H., et al.: Fast preparation procedure for large, flat cellulose and cellulose/inorganic nanopaper structures. Biomacromolecules. 11(9), 2195–2198 (2010)
51. Hollertz, R., Wågberg, L., Pitois, C.: Effect of composition and Morphology on the dielectric response of cellulose-based electrical insulation. IEEE Trans. Dielectr. Electr. Insul. 22(4), 2339–2348 (2015)
52. Johnson, R., Bhattacharyya, G.: Statistics: Principles and Methods, 6th edn. John Wiley & Sons. Inc. Hoboken (2010)
53. Lesaint, O., Costeanu, L.: Positive streamer inception in cyclohexane : evidence of formative time and cavitation process. In: Proceedings of the 19th IEEE International Conference on Dielectric Liquids (ICDL), pp. 29–32. ICDL, Manchester (2017)
54. Denat, A., Gosse, J.P., Gosse, B.: Electrical conduction of purified cyclohexane in a divergent electric field. IEEE Trans. Electr. Insul. 23(4), 545–554 (1988)
55. Jomni, F., Aitken, F., Denat, A.: Experimental investigation of transient pressure waves produced in dielectric liquids. J. Acoust. Soc. Am. 107(3), 1203–1211 (2000)
56. Davari, N., et al.: Field-dependent molecular ionization and excitation energies: implications for electrically insulating liquids. AIP Adv. 4(3), 037117 (2014)
57. Eriksson, G.: Easy evaluation of streamer discharge criteria. In: Proceedings of the COMSOL Conference, pp. 1–12. Milan (2012)

**How to cite this article:** Ariza, D., et al.: First-mode of negative streamers: inception at liquid/solid interfaces. High Volt. 6(6), 1069–1078 (2021). https://doi.org/10.1049/hve2.12105